Reference Point Projection Method for Improved Dynamics of Solar Array Hardware Emulation

Thusitha Wellawatta and Sung-Jin Choi
School of Electrical Engineering, University of Ulsan, KOREA

Abstract

Solar array simulator (SAS) is a special DC power supply that regulates the output voltage or current to emulate characteristics of photovoltaic (PV) panels. Especially, the control of SAS is a challenging task due to the nonlinearity in the output curve, which is dependent on irradiance as well as temperature and is determined by panel materials. Conventionally, both current-mode control and voltage-mode control should be alternated by partitioning the operating curve into multiple sections, which is not only for the measurement noise problem with the feedback sensing but also for the control stability issue near the maximum power point. However, the occurrence of transition among different controllers may deteriorate the overall performance. To eliminate the mode transitions, a novel single controller scheme has been introduced in this paper, where the reference operating projection technique enables simple, smooth and numerically stable control. Theoretical consideration on the loop stability issue is discussed and the performance is verified experimentally for the emulation of a PV panel data in view of stability and response speed.

1. Introduction

Since atmospheric conditions cannot be manipulated, it is usually difficult to conduct controlled experiments with real solar panels. Instead, a hardware equipment called a solar array simulator (SAS) is becoming popular in emulating characteristics of photovoltaic (PV) panels under various irradiance and temperature profiles. SAS is so flexible equipment that researchers can test solar power generation system by feeding sequences of pre-programmed environmental conditions into SAS. Furthermore, experiments can be repeatable without limitations in time and space. With an updated panel database, different types of panel can also be tested easily.

Basic large signal block diagram of SAS is shown in Fig. 1. It consists of a power converter, a SAS controller, and a SAS engine. The SAS engine generates the target control reference according to the panel data and atmospheric conditions. The SAS controller regulates the output voltage or current of the power converter, which delivers the output power to the load system such as a solar power inverter or battery charger.

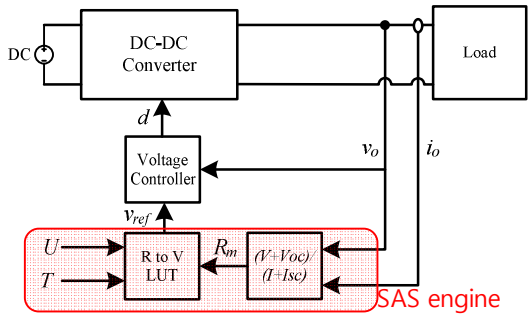

Fig.1. Large signal block diagram

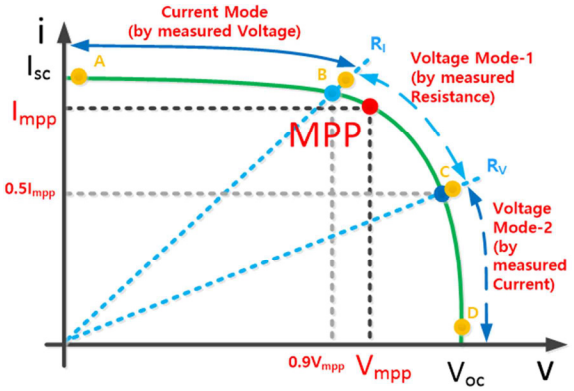

Fig.2. Conventional hybrid control method

The SAS engine contents panel data as a lookup table (LUT). For example, a three-dimensional table can generate a voltage reference, V_{ref}, for the voltage mode controller based on the sensed output current, I_{sense}. In the curve generation, the atmospheric information such as temperature, T, and irradiance, U, is also necessary. Eventually, the power stage is controlled by the set value of the simulator engine. According to physical properties of a photovoltaic cell, the shape of the I-V characteristic curve of the photovoltaic panel is non-linear as shown in Fig. 2. To emulate the curve, current mode control, or voltage mode control has been used in the conventional works. In case of current mode control, the current reference is generated from a LUT that maps from the sensed voltage, V_{sense}, to the reference current, I_{ref}, but the functionality is limited to the current source segment shown in Fig.2. The similar limitation confines voltage mode control to voltage source segment. In the literature [4], a graphical slope calculation predicts possible instability problems in the vicinity of the maximum power point (MPP) of the I-V curve for voltage mode as well as current mode control. Thus, both of these methods have poor performance in the vicinity of MPP.

As a solution, the hybrid control scheme is presented in the literature [4] [5]. The basic framework of this controller is shown in Fig. 2. Here, I-V curve of PV panel is partitioned into three regions. A new region is defined near MPP, where the output is controlled by a voltage mode control, but the reference voltage is calculated by an impedance measured as (1).

$$R_f = \frac{V_{sense}}{I_{sense}} \tag{1}$$

where, V_{sense} and I_{sense} are the sensing values of output voltage and current, respectively. However, since the impedance usually becomes either too large in the voltage source segment or too small in the current source segment to cover the entire I-V curve, such a hybrid control requires multiple controllers to be switched alternately. Thus, fluctuations in the output waveforms due to frequent transitions across the control boundaries may cause another problem.

2. Principle of Operation and Proposed Control Scheme

According to the above studies, current mode and voltage mode controller are suitable for current source section and voltage source section, respectively. It is noticeable that the limitation is originated from the feedback loop gain. In the SAS engine, the control reference signal is generated by the SAS output variable and it will define the outer feedback loop gain, which converts from the sensed signal to the reference signal. For example, the outer feedback gain is determined by the incremental slope of the I-to-V conversion LUT in the voltage mode control or that of the V-to-I conversion LUT in the current mode control. However, if the feedback gain is extremely reduced beyond their operating region as shown in Fig.3 (a), where the system becomes unstable and shows the poor dynamic response.

Our main research object is to develop a universal control scheme that extends the control range to the entire range of I-V curve in a simple and numerically stable manner. Impedance based control can be a viable solution to alleviate the problem caused by too small outer loop gain, the impedance mapping can be done as shown in Fig. 3 (b). It reflects that distinct reference values can be generated by impedance feedback. However, according to our observation, this method has a practical issue near the open circuit condition and short circuit condition. The measured impedance usually becomes either too large in the voltage source segment or too small in the current source segment. Near open circuit condition, the impedance reaches to extremely large value (near infinity) and system stability can be lost. A similar issue is occurred near short circuit condition when the impedance is approaching zero. Thus, our study answers to this issue by shifting the origin point as shown in Fig. 3 (c). The formation of the

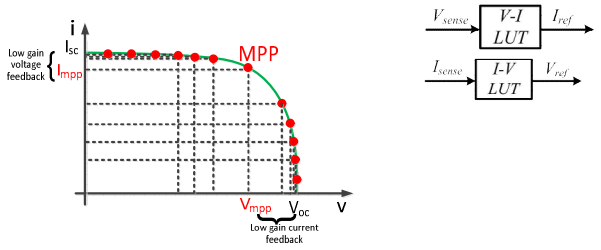

(a) Conventional current/voltage mode control

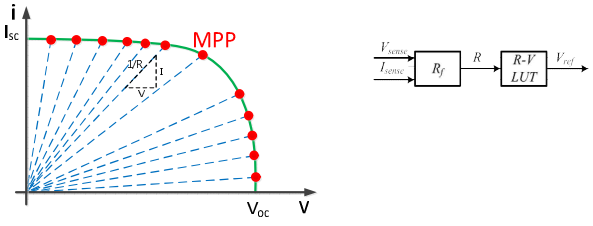

(b) Application of conventional impedance control to the entire region

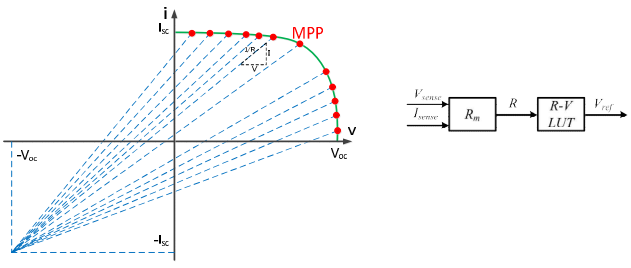

(c) Proposed operating point projection control

Fig.3. Graphical view of control methods

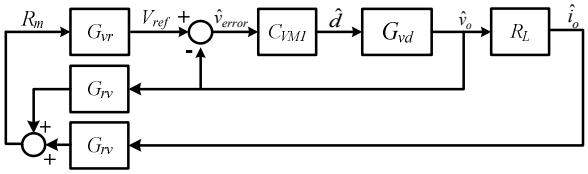

Fig.4. Small signal block diagram

modified impedance Rm is derived using (2).

$$R_m = \frac{V_{sense} + V_{oc}}{I_{sense} + I_{sc}} \tag{2}$$

where, V_{oc} is the open circuit and I_{sc} is the short circuit current in the standard test condition (STC). The shifting by V_{oc} and I_{sc} makes the feedback gain to be confined into a finite region that never become zero or infinity. This technique guarantees appropriate outer feedback gain to have stable operation in the entire I-V curve.

In the proposed scheme, the R-to-V conversion LUT is used to generate the reference voltage. The system small signal block diagram is shown in Fig. 4. Consequently, the LUT is developed according to the Rm. The voltage transfer function is derived as (3). The compensator can be designed considering the inner voltage loop (G_{vd}) and the outer loop gain. Transfer functions of voltage and current into resistance and Rm are defined (4), (5), and (6), respectively. Mathematical stability analysis and design procedure will be included in the full paper.

$$G_{vd}(s) = \frac{\hat{v}_o(s)}{\hat{d}(s)} \tag{3}$$

$$G_{rv} = \frac{\hat{r}_m}{\hat{v}_o} \tag{4}$$

$$G_{ri} = \frac{\hat{r}_m}{\hat{i}_o} \tag{5}$$

$$G_{vr} = \frac{\hat{v}_{ref}}{\hat{r}_m} \tag{6}$$

3. Performance Verification

To verify the performance of the proposed solar panel simulator, the simulation and hardware are implemented, and results are shown in Table 1. The system specifications are shown in Table 2. The system is tested on 1000W/m^2 insulations and 25^{0}C temperature. The schematic as shown in Fig.7 is used in the simulation and different loads are changed in 0.07th second in PSIM. Simulation waveforms of output voltage and current in the transience of RL=10Ω→20Ω is shown in Fig. 8. Vo, Io, and Rm are observed with the result of error around 1.2%.

The experiment is performed with a buck power converter and resistive loads as shown in Fig. 9. The SAS controller and SAS engine are implanted in a DSP. Load resistance is changed from 10Ω to 20Ω, and the waveforms of output voltage and current, voltage input of ACD in DSP, and the duty of buck converter are presented in Fig. 10. In the experiments, two active loads are parallel connected, and one load is activated after few seconds to obtain the transient. Numerical experiment results are also shown in Table 1 with the error below 3.5%. The accuracy of simulation and experiment has a slight difference because of noise. The proposed system settles the output value within 0.02s with very

low oscillation. These results prove that the proposed scheme could able to follow the datasheet values successfully and

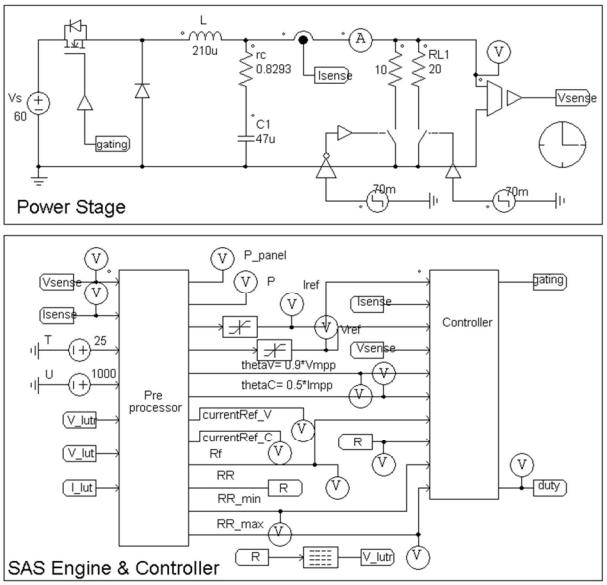

Fig.5. Solar Array Simulator using PSIM

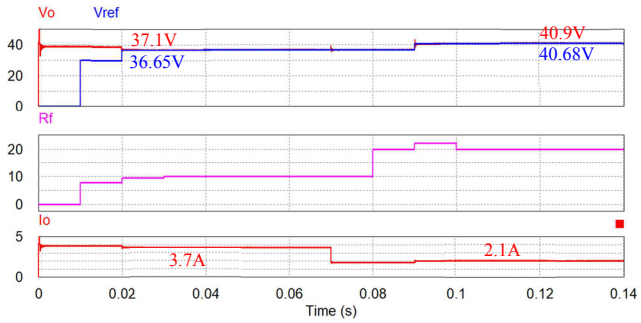

Fig.6. Simulation of RL=10Ω→20Ω transient

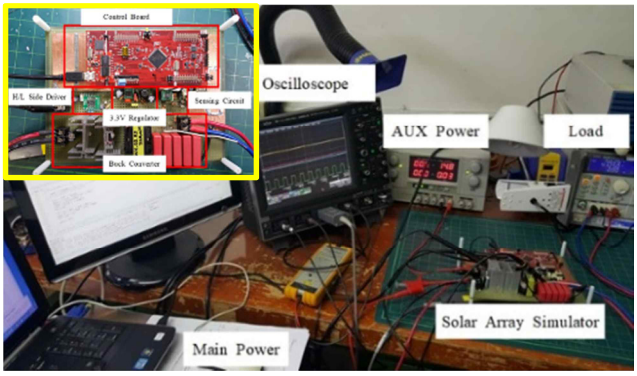

Fig.7. Experimental setup of solar array

performs enough speed and stability.

4. Conclusion

In this paper, a universal control scheme for the solar panel simulator is designed, analyzed and verified. To solve the stability problem of the conventional works, it utilizes an operating point projection technique to construct an R-to-V conversion LUT. The proposed scheme adopts a single controller with impedance feedback. The modified impedance is calculated by the operating point projection formula to have a finite outer feedback gain. The controller is designed by using the small-signal modeling and the system stability is mathematically analyzed. The simulation and experiment results show that control stability and response speed

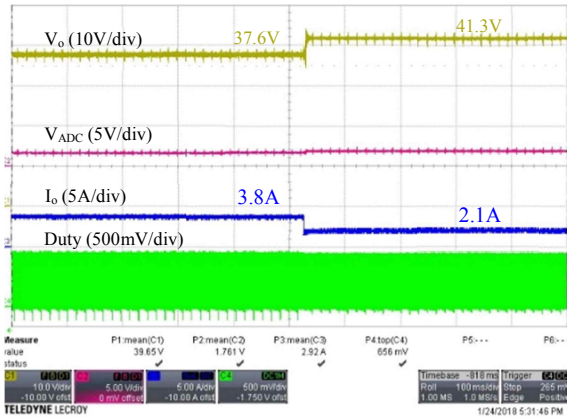

Fig.8. Experiment result of load change

of the solar array simulator are verified through real hardware implementation. In the final paper, detailed mathematical descriptions of the outer loop stability improvements and more hardware test results in the presence of maximum power point trackers will be included.

References

[1] D. Sera, R. Teodorescu, and P. Rodriguez, “PV Panel Model Based on Datasheet Values,” IEEE International Symposium on Industrial Electronics, pp. 2392-2396, 2007.

[2] Shlomo Gadelovits, Moshe Sitbon and Alon Kuperman, "Rapid Prototyping of a Low-Cost Solar Array Simulator Using an Off-the-Shelf DC Power Supply," IEEE Transactions on Power Electronics, Vol.29, NO.10, Oct.2014

[3] A.Vijayakumari, A.T.Devarajan and N.Devarajan, "Design and development of a model-based hardware simulator for photovoltaic array," Electrical Power & Energy Systems, 43(2012), p.40-46

[4] Y. Li, T. Lee, F. Z. Peng and D. Liu, "A Hybrid Control Strategy for Photovoltaic Simulator," 2009 24th Annual IEEE Applied Power Electronics Conf. and Expo., Washington, DC, 2009, pp. 899-903.

[5] I.D.G. Jayawardana, C.N.M. Ho, M. Pokharel, and G. Escobar, “A fast dynamic photovoltaic simulator with instantaneous output impedance matching controller,” 2017 IEEE Energy Conversion Congress and Exposition (ECCE), pp.5126 – 5132, 2017